Light-activation of the Archaerhodopsin H⁺-pump reverses age-dependent loss of vertebrate regeneration: sparking system-level controls *in vivo*

Dany Spencer Adams*, Ai-Sun Tseng*,‡ and Michael Levin§

Department of Biology and Tufts Center for Regenerative and Developmental Biology, Tufts University, 200 Boston Avenue, Suite 4600, Medford, MA 02155, USA

*These authors contributed equally to this work
‡Present address: School of Life Sciences, University of Nevada, Las Vegas, 4505 Maryland Parkway, Las Vegas, NV 89154-4004, USA
§Author for correspondence (Michael.Levin@Tufts.edu)

Summary

Optogenetics, the regulation of proteins by light, has revolutionized the study of excitable cells, and generated strong interest in the therapeutic potential of this technology for regulating action potentials in neural and muscle cells. However, it is currently unknown whether light-activated channels and pumps will allow control of resting potential in embryonic or regenerating cells *in vivo*. Abnormalities in ion currents of non-excitable cells are known to play key roles in the etiology of birth defects and cancer. Moreover, changes in transmembrane resting potential initiate *Xenopus* tadpole tail regeneration, including regrowth of a functioning spinal cord, in tails that have been inhibited by natural inactivity of the endogenous H⁺-V-ATPase pump. However, existing pharmacological and genetic methods allow neither non-invasive control of bioelectric parameters *in vivo* nor the ability to abrogate signaling at defined time points. Here, we show that light activation of a H⁺-pump can prevent developmental defects and induce regeneration by hyperpolarizing transmembrane potentials. Specifically, light-dependent, Archaerhodopsin-based, H⁺-flux hyperpolarized cells *in vivo* and thus rescued *Xenopus* embryos from the craniofacial and patterning abnormalities caused by molecular blockade of endogenous H⁺-flux. Furthermore, light stimulation of Arch for only 2 days after amputation restored regenerative capacity to inhibited tails, inducing cell proliferation, tissue innervation, and upregulation of *notch1* and *msx1*, essential genes in two well-known endogenous regenerative pathways. Electroneutral pH change, induced by expression of the sodium proton exchanger, NHE3, did not rescue regeneration, implicating the hyperpolarizing activity of Archaerhodopsin as the causal factor. The data reveal that hyperpolarization is required only during the first 48 hours post-injury, and that expression in the spinal cord is not necessary for the effect to occur. Our study shows that complex, coordinated sets of stable bioelectric events that alter body patterning—prevention of birth defects and induction of regeneration—can be elicited by the temporal modulation of a single ion current. Furthermore, as optogenetic reagents can be used to achieve that manipulation, the potential for this technology to impact clinical approaches for preventive, therapeutic, and regenerative medicine is extraordinary. We expect this first critical step will lead to an unprecedented expansion of optogenetics in biomedical research and in the probing of novel and fundamental biophysical determinants of growth and form.

Introduction

The use of light-activated ion-transporting proteins to alter transmembrane voltage is an important part of the field of optogenetics and has led to remarkable breakthroughs in our ability to elicit and inhibit action potentials in nerve and muscle cells (Knöpfel et al., 2010). However, it is unknown whether these tools are adaptable for use in developing or otherwise dynamic systems, especially during complex patterning and disease events (Levin, 2012). This is a critical issue as endogenous bioelectrical signals are known to regulate cellular processes including proliferation, differentiation, migration, and morphology (Levin, 2009). Thus biomedical applications that harness these processes by manipulating resting potential *in vivo*

can be facilitated by the flexibility of spatio-temporal control provided by optogenetics. Especially interesting is the potential applicability of this technology to regenerative medicine, where bioelectrical signals have been shown to initiate regeneration of complex, multi-tissue organs and appendages (Adams et al., 2007; Beane et al., 2011; Levin, 2012; Pai et al., 2012; Tseng et al., 2010).

A powerful model for studying regeneration of complex vertebrate structures is the *Xenopus* tadpole tail, which comprises spinal cord, notochord, muscle, nerves, vasculature, and skin. After tail amputation, the tail stump becomes highly depolarized. A bioelectrical hyperpolarizing signal is then required to initiate regeneration and is one of the earliest signals identified in this

process (Adams et al., 2007). Starting at 6 hours post-amputation (hpa), the proton pump H^+-V-ATPase is strongly expressed in the plasma membrane of the regeneration bud cells at the injury site. The H^+-V-ATPase-dependent H^+-efflux acts to repolarize the regeneration bud and this event is required to initiate proliferation, directed innervation, and induction of regenerative signaling pathways, leading to successful replacement of the missing tail (Tseng and Levin, 2012). Conversely, molecularly or chemically inhibiting H^+-V-ATPase activity blocks regeneration. Interestingly, *Xenopus* tadpoles exhibit age-dependent changes in regenerative ability similar to humans (Beck et al., 2003). The absence of endogenous H^+-efflux and the unrelieved depolarization of the tail stump inhibits regeneration during this age-specific physiological non-regenerative (also known as the "refractory") period of development (Adams et al., 2007).

We explored the ability of optogenetics to address two important unknowns. First, can a minimally invasive method be developed for precise control of bioelectric states of cells outside of the neuromuscular system *in vivo*? Second, because pharmacological reagents cannot be reliably washed out of 3-dimensional tissues, it is difficult to put a temporal boundary on the activity of membrane voltage in regenerative pathways. Given the ability of light-gated ion pumps to be regulated temporally, we hypothesized that using such a tool in regenerating cells could allow us to control the external manipulation of V_{mem} at precisely defined time points. As this approach has not yet been experimentally investigated, a successful result would: represent an important additional use for optogenetic methods, identify novel schemes for clinical therapies, and reveal new aspects of the mechanisms of bioelectrical regulation during development and regeneration.

To test the ability of a light-gated ion translocator to alter endogenous voltage and thereby induce regeneration in non-regenerative tadpole tails, and to further probe the temporal requirements of ion flows during regeneration, we employed Archaerhodopsin (Arch), a light-activated, hyperpolarizing H^+-pump (Chow et al., 2010) to manipulate H^+-flux-dependent initiation of regeneration. Here, we show that Arch acts in a light-dependent manner in larval *Xenopus* tissues *in vivo* to hyperpolarize cells, and thus can functionally replace the endogenous V-type proton pump. Light-activated Arch, functioning outside of the spinal cord, rescues both developmental and regenerative defects caused by age-dependent (endogenous) or experimental inhibition of normal H^+-efflux, and it acts through *Notch* and *MSX1*. Light-activation for only 48 hours post-injury, followed by continuous darkness, is sufficient to initiate the entire program of regeneration of this complex neuromuscular appendage at ages that otherwise would not regenerate.

Results

Absence of H^+ efflux induces developmental and regenerative defects

During *Xenopus* development, inhibition of H^+-V-ATPase function, molecularly or chemically, leads to both embryonic and regenerative defects (Fig. 1). Injection of mRNA encoding YCHE78, a dominant negative H^+-V-ATPase subunit, at the one cell stage results in craniofacial malformations including small branchial arches, and irregular eye, ear and olfactory bulb structure, (Fig. 1A–D). Treatment with concanamycin, a specific
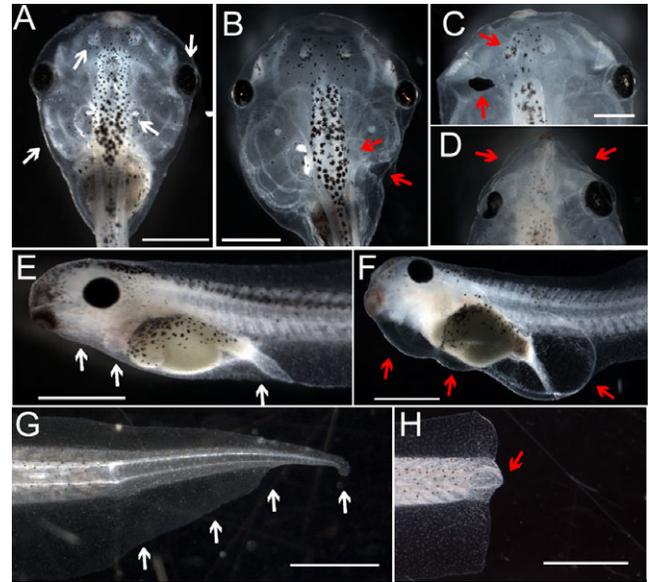

Fig. 1. Phenotypes caused by inhibition of the H^+-V-ATPase. (A) Dorsal view of normal stage 47 tadpole. White arrows indicate normal eyes, olfactory bulbs and branchial arches. **(B–D)** Craniofacial phenotypes commonly seen after injection at the one-cell stage with mRNA encoding YCHE78, a dominant negative H^+-V-ATPase subunit. B shows abnormally small branchial arches; the arrow in C points to ectopic pigments in the optic nerve; the arrows in D point to a missing eye and an abnormal olfactory bulb. Scale bar in C (for C and D)=0.5 mm. **(E)** Profile of a normal stage 42 embryo. Arrows for comparison with F. **(F)** Stereotypical swellings caused by incubation of tadpoles in 10 nM concanamycin for 24 hours following tail amputation at stage 40. Even if removed from concanamycin at this stage, all tadpoles subsequently die. Anterior is to the left and dorsal is up. **(G)** A regenerated tail shown approximately 8 days post-amputation. The amputation plane was just anterior to (to the left of) the leftmost white arrow. **(H)** A non-regenerating tail. After amputation at stage 47, this tail did not grow back, a characteristic of tails cut at this age that defines the refractory stage. The red arrow points to the area referred to as the regeneration bud; the amputation plane is immediately anterior. Except where noted, scale bars=1 mm.

chemical H^+-V-ATPase inhibitor, at an early tadpole stage causes edemas in the head and trunk and subsequent lethality (compare Fig. 1E,F). H^+-V-ATPase function is also required for initiating tadpole tail regeneration. During the refractory period, the absence of endogenous H^+-V-ATPase activity after tadpole tail amputation prevents regenerative regrowth (compare Fig. 1G,H). Together, these observed phenotypes demonstrate essential requirements for stable H^+ efflux in normal craniofacial development, osmotic balance, and tail regeneration.

The multiple roles of H^+ efflux during development and regeneration suggest that this ion current should be an important target for therapeutic manipulation of tissues. We therefore sought to identify optogenetic tools that induce stable, controllable H^+ efflux *in vivo* and to use an optogenetic approach to prevent developmental defects, correct ion imbalance, and initiate the restoration of a complex appendage, the tail.

The light-activated proton pump, Arch, is active in *Xenopus* cells

The Archaerhodopsin-3 (Arch) protein is a light-gated proton pump (Chow et al., 2010) that is active when expressed in neurons. To determine whether Arch is functional in *Xenopus* embryonic cells, we first examined Arch expression. After

injection of the Arch mRNA into early embryos, a linked fluorescent tag (GFP or Tomato) was imaged. Both epifluorescence and spinning disk confocal microscopy consistently detected strong Arch protein on cell surfaces from approximately the 32-cell (Fig. 2A) through tadpole stages (Fig. 2B,C), indicating that it is expressed as predicted.

To verify the light-dependent activity of Arch in *Xenopus* cells, we measured resting membrane voltage and intracellular pH *in vivo*. Impaling early embryonic cells showed the expected hyperpolarization of Arch-expressing light-stimulated cells (Arch+Light) relative to Arch-expressing, unstimulated cells maintained in the dark (Arch+Dark; -40 ± 7 mV *versus* -22 ± 8 mV; $n=12$, $t=3.541$, $P=0.002$) (Fig. 2D). To establish whether Arch-Tomato could pump H^+ ions out of cells, we measured intracellular pH under conditions when Arch was either inactive or active. BCECF is a fluorescent pH reporter whose excitation wavelengths do not strongly stimulate Arch (Fig. 2E). Using BCECF, we found that the difference between pH of cells expressing Arch-Tomato and those that are not expressing it was 0.3 ± 0.2 pH units on average (Fig. 2F,G,H). Using SNARF-5F, a fluorescent pH reporter whose excitation wavelengths maximally stimulate Arch and for which the irradiance of the illumination source used was higher than those used for BCECF, we found an average difference of 0.7 ± 0.3 pH units (Fig. 2I,J,K). These data confirm that Arch is activated by light to pump H^+ ions out of the minimally differentiated cells in the regeneration bud. Together, the V_{mem} measurements and the pH results establish that Arch functions in a light-dependent manner as a proton pump to increase polarization in *Xenopus* cells *in vivo*.

Light-induced Arch activity rescues developmental defects

Our experimental evidence suggests that Arch activity should be able to substitute for the function of H^+-V-ATPase, the endogenous proton pump, during development. To test whether light-illuminated Arch could in fact act as a gain of function tool to rescue deficiencies in H^+-flux regulation, we first examined the ability of active Arch to prevent embryonic defects caused by molecular inhibition of H^+-flux. As shown in Fig. 1, expression of YCHE78 blocks endogenous H^+-V-ATPase function resulting in patterning and craniofacial abnormalities (Vandenberg et al., 2011). Consistent with restoration of H^+ efflux by light-activated Arch, raising embryos expressing both YCHE78 and Arch under light prevented those developmental defects, as well as lethality, as compared to sibling embryos raised in the dark, ($n=149$, $Z=3.423$, $P<0.001$). Similarly, edemas induced by concanamycin treatment at the tadpole stage (Fig. 1F) were also suppressed by concurrent Arch activation via light treatment. Thus Arch activity functionally replaced the normal H^+ efflux during development and suppressed embryonic defects and physiologic imbalance.

Light-induced Arch activity initiates regeneration

Having demonstrated that Arch functions in non-excitable embryonic tissues to suppress defects caused by molecular inhibition of H^+-V-ATPase, we sought to test the therapeutic potential of using this approach to induce vertebrate regenerative repair. During the refractory period, tadpoles exhibit human-like age-dependent regenerative ability: tail regeneration is endogenously blocked during one phase of tadpole development, just as digit regeneration is endogenously blocked in children over the age of seven (Douglas, 1972; Illingworth, 1974; Illingworth and Barker, 1980). To test whether Arch activity could reverse this natural inhibition, we asked
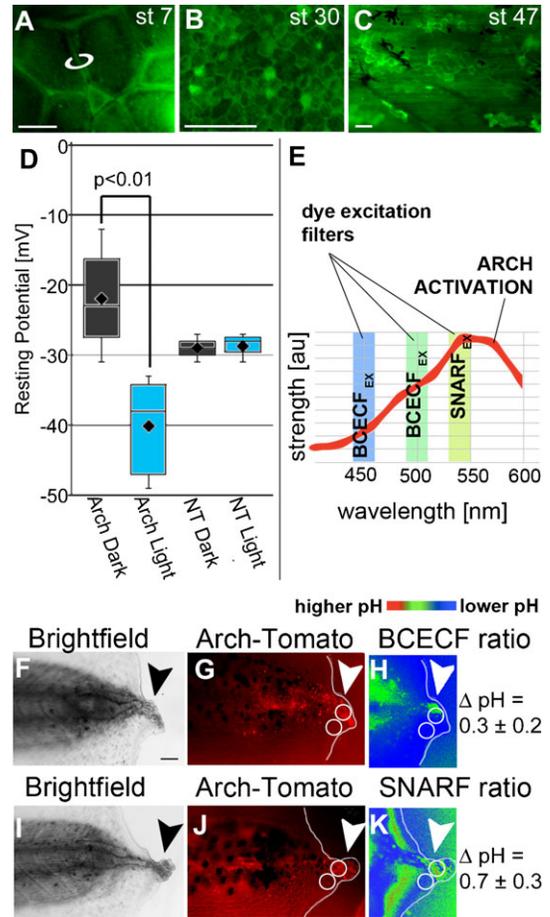
Fig. 2. Arch is expressed and can be activated in *Xenopus* cells.
(**A–C**) Expression of Arch-GFP at the stages indicated. mRNA for Arch-GFP was injected at the one cell stage and lasts for at least the 8 days required for the longest experiments. (A) View of animal pole of a Stage 7 embryo, the stage at which electrophysiology was performed. Arch-GFP expression is especially visible at cell–cell boundaries (e.g. white circle) where the cells have less pigment. (B) Arch-GFP is still present in the membranes of hexagonally-packed ectodermal cells at stage 30, well after the developmental stages that are relevant for craniofacial development. (C) Arch-GFP is still strongly expressed at stage 47, the refractory stage, during which, if the tail is cut, it does not grow back due to endogenous inhibition. The black arborized cells are melanophores, the longer aligned cells are muscle cells, and the hexagonally arrayed cells are epidermis. (**D**) Resting potential (V_{mem}) of impaled cells in embryos at stage 7. Arch-tomato was injected at 1 cell, then half of these embryos and half of the uninjected (NT=no treatment) controls were placed under blue light while the other halves were kept in the dark until stage 7. The V_{mem} of untreated embryos was about -29 ± 2 mV and was unaffected by light. Arch-injected embryos kept in the dark were depolarized while Arch-injected embryos kept in the light were hyperpolarized. (**E**) Explanation of pH measuring experimental protocol. Two dyes were used to compare pH of Arch-tomato expressing cells with pH of cells showing no expression. BCECF is excited by 450 and 500 nm light, which does not activate Arch very strongly, while SNARF-5F is excited by 540 nm, which maximally activates Arch. The prediction is that the pHs measured by BCECF will differ by less than the pHs measured by SNARF because Arch should be maximally activated under the latter conditions, thus causing pH to increase in Arch expressing cells. (**F–K**) Results of pH measurements using two dyes. (F,I) Brightfield images showing positions of regeneration buds. (G,J) Images of Arch-tomato fluorescence used to choose regions of interest (ROIs) defined by high and low tomato fluorescence. (H,K) ROIs from G and J were transferred to the ratio images generated by the dyes (see Materials and Methods). As predicted, measurements made under low Arch-activation conditions (BCECF, F–H) show only a 0.3 ± 0.2 pH unit difference between Arch-tomato expressing and non-expressing cells. In contrast, under Arch-activating conditions (SNARF-5F, I–K), the pH difference is approximately doubled to 0.7 ± 0.3 pH units. Anterior is to the left in all images except A. Scale bars=100 μm.

whether light-activated Arch H$^+$ pump activity can initiate regeneration during the refractory period.

Arch-Tomato mRNA was injected into early embryos and the embryos were allowed to develop in darkness. During the refractory period, tadpole tails were amputated and immediately placed either under light or in the dark for 2 days and then further grown in the dark for 5 additional days. We found that the age-specific refractory inhibition of regeneration was reversed in light-stimulated Arch-expressing tadpoles but not in unstimulated Arch-expressing tadpoles, with light approximately doubling regenerative ability ($n = 16$ groups representing 428 tadpoles total, $t = 3.709$, $P = 0.002$) (Fig. 3A; supplementary material
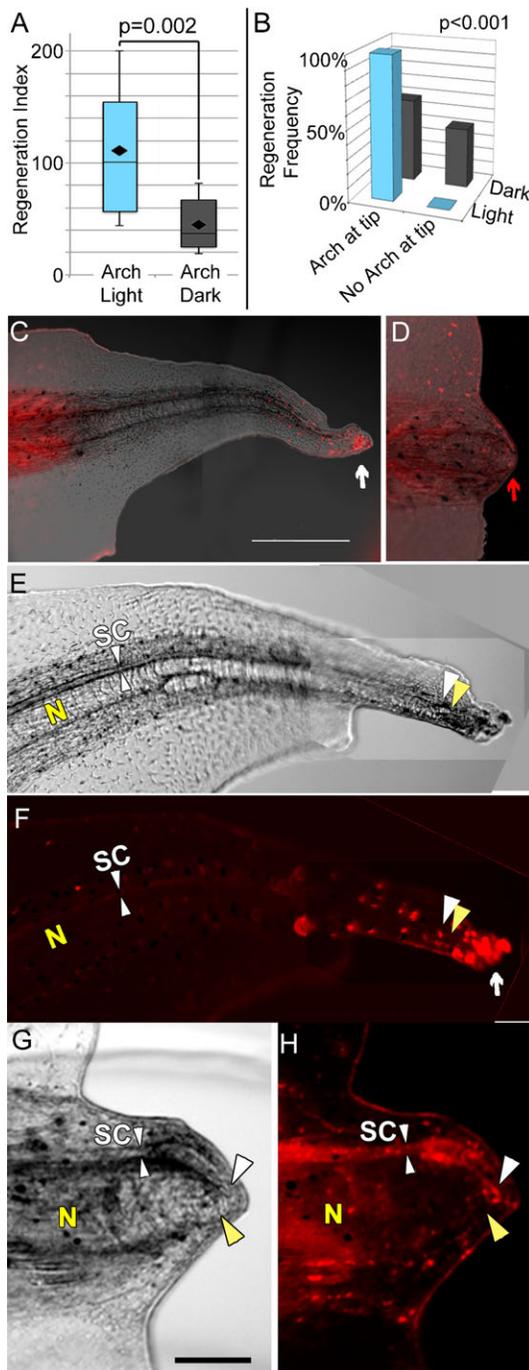
Table S1). Moreover, in contrast to previous results showing that constitutive H$^+$-efflux both before and after amputation could lead to refractory regeneration, here we initiated hyperpolarization only *after* amputation, a more relevant model for clinical applications, and for only 2 days. Importantly, after 2 days of light exposure, Arch activity did not cause any side effects such as tissue abnormalities.

To better characterize the role of Arch activity in the light-induced refractory regeneration, we examined the spatial distribution of Arch expression in regenerated and non-regenerated tails. Concentrated Arch expression (as evidenced by the presence of Tomato fluorescence) was seen at the distal tip of all of the successful tail regenerates after light stimulation (Fig. 3B,C). Non-regenerated tail stumps, in contrast, showed randomized regions of Arch expression. Similarly, no correlation between Arch localization and regenerative success was observed in tails of tadpoles expressing Arch but grown in the dark (Fig. 3D).

For successful regeneration to occur, proper nerve patterning is essential, so we examined whether Arch expression correlated with the position of neurons. Surprisingly, expression of Arch-Tomato in the spinal cord was not required for full regeneration (Fig. 3E,F). Consistent with this observation, amputated tail stumps that contained strong Arch-Tomato expression in the neural tissue, but lacked strong distal expression, failed to regenerate after light activation (Fig. 3G,H). Our data establish that temporally inducing H$^+$ efflux via Arch activation after refractory tail amputation is sufficient to initiate regeneration during this endogenous non-regenerative state. Furthermore, Arch activity is not required in the neural cells of the amputated tail stump, but rather in a small distal population.


Fig. 3. Arch-Tomato activity promotes regenerative repair.
(**A**) Comparison of regeneration indices, a measure of regeneration success, of the tails of Arch-Tomato expressing tadpoles amputated at the refractory stage. Significantly better regeneration was found in tadpoles that were exposed to Arch-activating light for 48 hours following amputation relative to those kept in the dark (*t*-test). (**B**) Comparison of localization of Arch-Tomato in tadpoles exposed to dark *versus* light for 48 hours post-amputation. Under Arch-activating light, regeneration correlated perfectly with the presence of a group of Arch-Tomato expressing cells at the very tip of the regenerating tail (see C below). In contrast, among the tadpoles kept in the dark, regeneration success did not correlate at all with localization of Arch-tomato. The distributions are highly significantly different (χ^2). (**C**) Arch-Tomato localization in a regenerated tail 8 days after amputation at the non-regenerative stage 47. Arch-Tomato expression is still strong in the uncut part of the tail to the left, and in a small clump of cells at the distal most tip of the regenerating tail (white arrow). Otherwise, as expected, there is very low if any expression of Arch-tomato in the regenerate. Scale bar = 100 µm. (**D**) Arch-Tomato expression in a tail that did not regenerate. While there is expression all the way to the distal edge of the amputation plane, expression is relatively even, that is, there is no group of particularly bright cells. Scale bar as in C. (**E–H**) Higher magnification brightfield and fluorescence views of light-stimulated tails and Arch-Tomato expression. Yellow Ns indicate the notochords. White SCs and small arrowheads indicate the spinal cord. Letters were positioned on the brightfield images then transferred to the fluorescence images. At the distal ends (to the right) larger arrowheads indicate the posterior extents of the notochord (yellow) and spinal cord (white). Scale bars = 25 µm. (E,F) Brightfield and fluorescence images of a regenerated tail showing the bright cells to be further distal, and largely ventral, to the spinal cord. The bright cells are indicated by a white arrow in F. (G,H) A refractory tail that did not regenerate showing Arch-tomato expressing neural tissue extending to the distal tip of the non-regenerating bud. For all images, anterior is to the left and dorsal is up.

pH change alone is not sufficient to restore regeneration

Since Arch function modulates both, V_{mem} and pH, we sought to determine which of these physiological properties was causal in initiating regeneration. Previous data already showed that cellular hyperpolarization (using a chloride transporter, independently of proton flux) is sufficient to induce regeneration (Tseng and Levin, 2012). Thus, we asked whether pH change alone would improve regenerative response. To alter pH without changing V_{mem}, embryos were injected with mRNA encoding constitutively active NHE3, an electroneutral Na^+/H^+ exchanger

(Praetorius et al., 2000; Sabirov et al., 1999). Incubation of these embryos in culture medium containing high $[Na^+]$ that facilitates H^+-efflux through this antiport should, like Arch activity, raise internal pH but unlike Arch activity, should not affect V_{mem}. In the tail regeneration rescue assays performed during the non-regenerative refractory period, comparisons of NHE3-expressing tadpoles in high $[Na^+]$ medium to those in normal medium or to uninjected controls in either high $[Na^+]$ or normal medium gave no evidence of improved regenerative ability (total $n=255$, Kruskal–Wallis plus Dunn's Q, $P>0.5$ for all comparisons). We interpret these results to be inconsistent with a model in which an increase in pH is sufficient to induce refractory regeneration. Together with the evidence that shows V_{mem} change alone is sufficient to rescue refractory regeneration (Tseng and Levin, 2012), we conclude that it is principally the effect of light-stimulated Arch on V_{mem}, not on pH, that initiates regeneration.
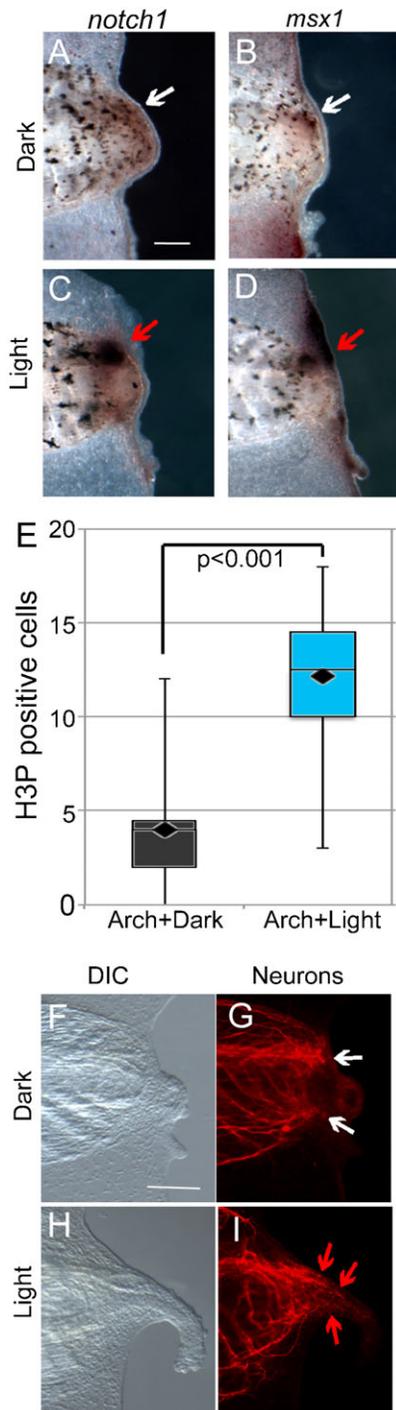
Stimulation of Arch-dependent H^+-efflux restores regeneration by triggering endogenous downstream genetic mechanisms

Because Arch activity restored refractory regeneration, we examined the potential downstream mechanisms by which this process was carried out. Notch1 and Msx1 are two well-characterized biochemical signaling components that are required to drive regenerative outgrowth and patterning (Beck et al., 2003). We asked whether Arch promoted tail regrowth by acting through these known downstream regenerative pathways. *In situ* hybridization revealed that light stimulation of Arch induced upregulation of both *Notch1* and *Msx1* (Coffman et al., 1990; Feledy et al., 1999) (Fig. 4A,B as compared to Fig. 4C,D). We also examined the effect of Arch stimulation on cell proliferation and nerve patterning, two processes that are required for regeneration. Light-dependent Arch activation more than doubled the number of mitotic cells in the tail regeneration bud region ($n=22$, $t=5.273$, $P<0.001$) (Fig. 4E) and promoted proper nerve patterning (compare Fig. 4F,G to Fig. 4H,I). Together, these results show that Arch-induced H^+ efflux initiates regenerative tail growth through endogenous mechanisms.

Discussion

In this study, we asked whether an optogenetic strategy could successfully initiate regeneration of a complex vertebrate structure *in vivo*. Previous work from our laboratory has demonstrated that a specific early proton efflux generated by

Fig. 4. Endogenous regenerative pathways follow arch activation by light. (**A–D**) Whole-mount *in situ* hybridizations for Notch1 and Msx1, components of regeneration signaling pathways. (A,B) Expression in the regeneration buds of Arch-tomato injected embryos maintained in the dark (white arrows). (C,D) Expression in the 3 days post-amputation (dpa) regeneration buds of Arch-Tomato injected embryos maintained in the light for 48 hours after amputation (red arrows). Expression is much higher in the light-stimulated tails.
(**E**) Comparison of the number of cells positive for phospho-histone H3 (H3P, a marker of mitotic activity) in the regeneration buds of Arch-tomato expressing tails kept in the dark *versus* the light. There were significantly more in the light-stimulated tails (*t*-test). (**F–I**) DIC and fluorescence images of α-tubulin (a neuronal marker) of Arch-Tomato expressing tails at 3 dpa. Tadpoles were kept in the dark *versus* the light for 48 hpa. (F,G) Non-regenerating tails kept in the dark show the typical arrangement of neurons that have stopped growing or grown in a curve towards the midline. (H,I) Regenerating tails kept in the light show the normal arrangement of neurons in a regenerating tail that is growing parallel to the AP axis of the tail and extending into the growing tail, although not reaching all the way to the distal tip. In all images, anterior is to the left and dorsal is up. Scale bars=25 μm.
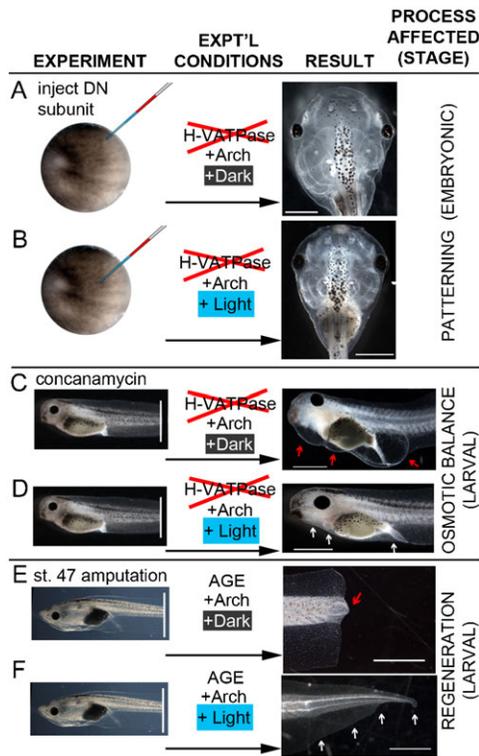
Fig. 5. Summary of the effects of light activation of Arch-tomato on embryos with blocked H⁺-V-ATPase. (**A**) Embryos expressing a dominant-negative H⁺-V-ATPase subunit develop severe craniofacial defects. (**B**) Illuminating co-expressed Arch-tomato from stage 9 to stage 26 significantly reduces the number of craniofacial abnormalities. (**C**) Embryos exposed to the highly specific H⁺-V-ATPase inhibitor concanamycin for 24 hours after amputation at stage 40 develop stereotypical swellings then die, consistent with an effect on osmotic balance regulation. (**D**) Illuminating Arch-tomato during exposure to concanamycin prevents swelling and subsequent mortality. (**E**) Tadpole tails amputated at stage 47 normally do not regenerate. (**F**) Illuminating Arch-tomato for 48 hours after amputation significantly increases the number of regenerating tails if there is a small group of Arch-expressing cells at the distal most tip of the tail. Scale bars=1 mm.

the V-ATPase H⁺ pump at the amputation site is required to initiate *Xenopus* tail regeneration, while inactivation of V-ATPase function in amputated tail stumps leads to regenerative failure. As proof-of-concept, we demonstrate that the light-gated H⁺ pump, Archaerhodopsin, can be expressed in non-excitable embryonic and tail cells of *Xenopus laevis* and it hyperpolarizes those cells when exposed to light (Fig. 2). Furthermore, we show that light-activated Arch activity restores regeneration in the absence of endogenous H⁺ efflux (Fig. 3). Exploiting the temporal control of Arch afforded by its light-sensitivity, we establish that the duration of H⁺-flux needed to start the regeneration pathway need not be long term, and, importantly for future biomedical use, that H⁺-efflux therapy can begin *after* amputation. Consistent with the known role of voltage-mediated early steps in regeneration, light-activated Arch signals upstream of canonical pathways required for tail regrowth (Fig. 4). Importantly, it overcomes the chemical and molecular inhibition of endogenous H⁺-flux and, notably, the physiological inhibition of regeneration such as is found in humans. To our knowledge, these are the first data to demonstrate that an optogenetic approach is feasible and useful in developing and regenerative systems *in vivo*, and that it can successfully

trigger normal biochemical signaling pathways downstream of bioelectric triggers.

Prior to measuring V_{mem}, Arch-expressing embryos were incubated under the light or in the dark, but then were kept at ambient light for up to 15 minutes prior to being measured. Thus, the average relative hyperpolarization of 22 mV caused by light-stimulation of Arch was stable for at least that long, or even more pronounced before the time spent at ambient conditions. This outcome highlights a critical difference between the cells under investigation here and the previously reported kinetics of Arch activation, where the assay for activity is inhibition or stimulation of an action potential lasting milliseconds. Specifically, the change in V_{mem} that is initiated by Arch stimulation is sustained for a much longer time.

Light activation of Arch induces a H⁺-flux. Consistent with this function, our results showed that light-activated Arch alters both V_{mem} and pH in *Xenopus* cells. Changes in V_{mem} correlate with tadpole regenerative ability whereas a role for pH in regeneration has not been documented. To address this question we changed V_{mem} and pH individually, to see whether either alone was sufficient for inducing regeneration. We recently showed that altering V_{mem} by the use of an exogenous chloride channel is sufficient to regulate regenerative ability in tadpoles (Tseng and Levin, 2012). Here, we report that expression of NHE (a sodium-proton exchanger that produces the pH gradient by an electroneutral process), which tested the role of pH without a concomitant V_{mem} change, induced no improvement of regeneration. Combined, these results suggest that it is unlikely that pH is a critical part of the mechanism for the initiation of regeneration and implicate the voltage change induced by Arch as the key causal factor.

We also discovered that age-dependent regeneration rescue by light-stimulated H⁺-pumping only occurs in tails with small populations of Arch-expressing cells at the distal tip of the tail; furthermore, there is no correlation between the position of these cells and the positions of neural tissue. Correct nerve patterning has been shown to be necessary for full regeneration; however, the presence of Arch-expressing cells in distal, non-neuronal cells of regenerates is more highly correlated with stimulation of regeneration, as well as with normal growth of the neurons along the anterior–posterior axis. As H⁺-V-ATPase is not expressed in the spinal cord ampullae after tail amputation, these data suggest that the repolarization of regeneration bud cells through H⁺-efflux is likely acting non-cell autonomously to drive regeneration of neural tissue and then the tail. The development of tissue-specific tools in *Xenopus* will enable us to further address this question in the future.

The data revealed several important new aspects of bioelectric control of regeneration. First, the light stimulation was stopped precisely at 48 hours post-injury; reliable wash-out of pharmacological inhibitors or inactivation of misexpressed genes cannot be done in this system, and these data demonstrated that hyperpolarization during the first 2 days is sufficient to induce the entire complex, highly coordinated, self-limiting 7-day cascade of tail rebuilding. Second, it was seen that function of *Arch* in the spinal cord was not required for regeneration (Fig. 3C,D). Given the known importance of nerve supply for regeneration (Gaete et al., 2012; Thornton, 1970), it is important for the development of biomedical strategies to note that bioelectric stimulation of other tissues can induce a strong repair program. Finally, we showed that optogenetic induction of

regenerative repair activates known transcriptional cascades (Fig. 4) and can thus potentially be used to regulate these pathways in multiple contexts.

In summary, we utilized the temporal activation of an ion current via a light-gated pump to initiate coordinated system-level changes to prevent craniofacial malformations or restore age-dependent loss of regenerative ability (Fig. 5). Instead of controlling animal behavior or spiking in the CNS or muscle, our study indicates that it is possible to affect fundamental alteration in body structures, without adversely affecting overall development, by manipulation of bioelectrical signals. This finding has important implications since ion transport is well-known for being essential not only for excitable cell behavior, but also for the body's anatomical homeostasis. Furthermore, the regulation of ion flux has increasingly been identified as a critical player in diseases including cancer. Moreover, there have recently been concerns raised about the safety of proton pump inhibitors taken during pregnancy and their links to resulting birth defects (Gill et al., 2009; Pasternak and Hviid, 2010). Our application of optogenetics to the control of complex developmental and regenerative bioelectrical events, and the regulation of known transcriptional cascades by brief optical stimulation of cells demonstrates the enormous potential for expanding the use of light-controlled ion flux beyond regulating action potentials in nerve and muscle tissues. Indeed, there is tremendous potential to address questions about ion-flux based disease, such as cancer, and especially for new approaches in regenerative medicine.

Materials and Methods
Xenopus husbandry and experimentation
This study was carried out in strict accordance with the recommendations in the Guide for the Care and Use of Laboratory Animals of the National Institutes of Health. The protocol was approved by Tufts University's Institutional Animal Care and Use Committee (Tufts IACUC protocol #M2011-70). Embryos were collected and maintained as described previously (Sive et al., 2000) and grown in $0.1\times$ Modified Marc's Ringers (MMR). Staging was according to Nieuwkoop and Faber (Nieuwkoop and Faber, 1967). Tail amputation was performed at stage 47 (a refractory stage) for physiological inhibition, as described previously (Adams et al., 2007; Tseng et al., 2010). For molecular studies, *Xenopus* embryos were fixed overnight in MEMFA (Sive et al., 2000). *In situ* hybridization was carried out according to standard protocols (Harland, 1991) with probes to *Notch1* (Coffman et al., 1990), and *Msx1* (Feledy et al., 1999). Antibodies used were anti-acetylated α-tubulin (Sigma #T6793), and anti-phospo-histone-3 (H3P; Upstate #05-598) at 1:1000 dilution.

mRNA injection
Arch-GFP or Arch-Tomato was injected at 60 ± 10 pg; this dose was determined to have activity without causing lethality. Because of the very low salinity of MMR, other candidate hyperpolarizing optogenetic reagents were found to be unsuitable for this system; additionally, no optogenetic reagent that can depolarize embryonic or ectodermal *Xenopus* cells were found in our testing of dozens of optogenetic protein constructs. Injection of 4 ± 1 ng of YCHE78 mRNA at the one cell (fertilized egg) stage caused both left–right patterning defects and craniofacial abnormalities. For molecular inhibition rescue, 60 ± 10 pg of Arch-Tomato mRNA was co-injected with the YCHE78 mRNA (Adams et al., 2007). For the NHE3 experiments, because intracellular $[Na^+]$ in blastomeres is higher than $[Na^+]$ of MMR (21 mM *versus* 9.9 mM), $0.1\times$ MMR was supplemented with 42 mM Na-gluconate to facilitate activity of the NHE3 antiporter.

Light treatment
Light treatment consisted of placing Petri dishes of tail-amputated tadpoles either (a) beneath an array of six LEDs (471 nm) at a distance resulting in irradiance of 0.5 ± 0.1 mW/mm^2 or (b) into a light-tight box containing two fiber optic cables connected to SugarCube LEDs (Boston Engineering, Waltham, MA) delivering 0.8 ± 0.1 mW/mm^2 of 463 nm light. To prevent phototoxicity and heating of the medium during the 48 hours of exposure, dishes were placed on cooling stages to maintain the temperature between 18 and 20℃ and lights were repeatedly turned on for 500 milliseconds then off for 2 seconds. All dark control dishes were kept at

a similar temperature, but under a light blocking cover. After 2 days, tadpoles were transferred to fresh $0.1\times$ MMR at 22℃, then scored 5 days later. Prior to direct measurement of membrane voltage (V_{mem}) by impaling with a microelectrode, the light regime was altered to 5 seconds on then 10 seconds off to insure that Arch was active and could be light-stimulated before cells were too small.

pH measurements
Tails of Arch-Tomato expressing stage 47 tadpoles were amputated. Four days later, after incubation in the light, tadpoles were incubated in 5 μM 2′,7′-Bis-(2-Carboxyethyl)-5-(and 6)-Carboxyfluorescein, Acetoxymethyl Ester (BCECF-AM) or Semi-Naphthyl Rhodofluor-5 Acetoxymethyl Ester (SNARF-5F) for 2 hours. Excess dye was washed out, then the embryos were lightly anesthetized with 0.15% MS222 and imaged. Measurements were made using an Olympus BX-61 with epifluorescence optics; illumination was from a Lumen200 metal halide lamp. To image BCECF, a dual excitation dye, filters were EX 450/20, D 460, EM 535/30 (the isobestic point) and EX 500/20, D 515, EM 535/30. To image SNARF-5F, a dual emission dye, filters were EX 540/25, D 565 and D 610, and EM 580/25 (the isoemissive point) or EM 640/25. Metamorph software was used to perform darkfield and flatfield corrections and to create ratio images, 500/450 for BCECF and 640/580 for SNARF-5F. Images were transferred to Photoshop™ with no changes to pixel intensities and the histogram function was used to calculate means and standard deviations of pixel intensities in regions of interest (ROIs) chosen on images of Arch-tomato fluorescence then transferred to the ratio images. Conversion from differences in intensity to differences in pH were made using conversion data from the literature (Morley et al., 1996; Sasaki et al., 1992).

Electrophysiology
V_{mem} was measured directly using a Warner Instruments Oocyte Clamp Amplifier model OC-725C with oocyte pathclamp model 7251.I (Harvard Apparatus Company, Hampden, CT). Borosilicate microelectrodes (O.D. 1.0 mm, I.D. 0.50 mm) were pulled on a Sutter Instruments Flaming Brown P-97 micropipette puller ($P=500$; heat=257; pull=60; vel=100; time=200) and the tips were broken by hand. Electrodes were filled with 2M KCl and the embryos were bathed in $0.1\times$ MMR. Embryos that had been injected with Arch mRNA at the one cell stage, then kept under light or in the dark, were moved to the rig and kept under ambient light for up to 15 minutes prior to, and then during, measurement.

Scoring of regeneration efficiency
Regenerative ability was quantified by examining the amputated tails 7 days after amputation. A scoring system was used to divide the tadpoles into four categories: no, bad, good, and full regeneration, as described previously (Adams et al., 2007). Regenerative ability was then summarized as a score called the Regeneration Index, with 0 indicating no regeneration of any individual and 300 indicating full regeneration of all animals. YCHE78's effect on development was scored by dividing embryos into three categories: normal patterning and face; heterotaxia (abnormal left–right positioning of the gut, gall bladder or heart loop) and/or craniofacial abnormalities; or dead.

Microscopy
Fluorescence microscopy was performed on an Olympus BX-61 compound microscope using, for Arch-GFP EX470/20, D485, EM517/23, and for Arch-tomato EX545/20, D565, EM595/50. For lower magnification/resolution images, a Nikon SMZ-1500 with epifluorescence optics and similar filter sets was used.

Statistics
All tests on optogenetic constructs compared the light *versus* dark treatments. The effects of light and dark in the absence of Arch (no Arch controls) were compared separately and showed no differences (supplementary material Table S1). *T*-tests were used to compare the results of electrophysiological measurements, physiological inhibition experiments, and numbers of H3P-positive cells. A Mann–Whitney U test was used to compare the distributions of wild-type, abnormal, and dead tadpoles resulting from YCHE78 injection. For Arch activity, the number of H3P-positive cells, and Arch+YCHE sample sizes were the number of individual tadpoles. To compare regeneration indices (regeneration ability) after refractory amputation, the sample sizes were the number of dishes, which collectively represented 428 tadpoles. The effects of NHE by $[Na^+]ext$ were compared using a Kruskal–Wallis test followed by Dunn's Q to identify pairwise significant differences.

Competing Interests

The authors have no competing interests to declare.

References

Adams, D. S., Masi, A. and Levin, M. (2007). H$^+$ pump-dependent changes in membrane voltage are an early mechanism necessary and sufficient to induce *Xenopus* tail regeneration. *Development* **134**, 1323-1335.

Beane, W. S., Morokuma, J., Adams, D. S. and Levin, M. (2011). A chemical genetics approach reveals H,K-ATPase-mediated membrane voltage is required for planarian head regeneration. *Chem. Biol.* **18**, 77-89.

Beck, C. W., Christen, B. and Slack, J. M. (2003). Molecular pathways needed for regeneration of spinal cord and muscle in a vertebrate. *Dev. Cell* **5**, 429-439.

Chow, B. Y., Han, X., Dobry, A. S., Qian, X., Chuong, A. S., Li, M., Henninger, M. A., Belfort, G. M., Lin, Y., Monahan, P. E. et al. (2010). High-performance genetically targetable optical neural silencing by light-driven proton pumps. *Nature* **463**, 98-102.

Coffman, C., Harris, W. and Kintner, C. (1990). Xotch, the Xenopus homolog of Drosophila notch. *Science* **249**, 1438-1441.

Douglas, B. S. (1972). Conservative management of guillotine amputation of the finger in children. *Aust. Paediatr. J.* **8**, 86-89.

Feledy, J. A., Beanan, M. J., Sandoval, J. J., Goodrich, J. S., Lim, J. H., Matsuo-Takasaki, M., Sato, S. M. and Sargent, T. D. (1999). Inhibitory patterning of the anterior neural plate in *Xenopus* by homeodomain factors Dlx3 and Msx1. *Dev. Biol.* **212**, 455-464.

Gaete, M., Muñoz, R., Sánchez, N., Tampe, R., Moreno, M., Contreras, E. G., Lee-Liu, D. and Larraín, J. (2012). Spinal cord regeneration in *Xenopus* tadpoles proceeds through activation of Sox2-positive cells. *Neural Dev.* **7**, 13.

Gill, S. K., O'Brien, L., Einarson, T. R. and Koren, G. (2009). The safety of proton pump inhibitors (PPIs) in pregnancy: a meta-analysis. *Am. J. Gastroenterol.* **104**, 1541-1545, quiz **1540**, 1546.

Harland, R. M. (1991). *In situ* hybridization: an improved whole mount method for *Xenopus* embryos. In *Xenopus Laevis: Practical Uses In Cell And Molecular Biology* (*Methods In Cell Biology, Vol. 36*) (ed. B. K. Kay and H. B. Peng), pp. 685-695. San Diego (CA): Academic Press.

Illingworth, C. M. (1974). Trapped fingers and amputated finger tips in children. *J. Pediatr. Surg.* **9**, 853-858.

Illingworth, C. M. and Barker, A. T. (1980). Measurement of electrical currents emerging during the regeneration of amputated finger tips in children. *Clin. Phys. Physiol. Meas.* **1**, 87.

Knöpfel, T., Lin, M. Z., Levskaya, A., Tian, L., Lin, J. Y. and Boyden, E. S. (2010). Toward the second generation of optogenetic tools. *J. Neurosci.* **30**, 14998-15004.

Levin, M. (2009). Bioelectric mechanisms in regeneration: unique aspects and future perspectives. *Semin. Cell Dev. Biol.* **20**, 543-556.

Levin, M. (2012). Molecular bioelectricity in developmental biology: new tools and recent discoveries: control of cell behavior and pattern formation by transmembrane potential gradients. *Bioessays* **34**, 205-217.

Morley, G. E., Taffet, S. M. and Delmar, M. (1996). Intramolecular interactions mediate pH regulation of connexin43 channels. *Biophys. J.* **70**, 1294-1302.

Nieuwkoop, P. D. and Faber, J. (1967). *Normal Table Of Xenopus Laevis (Daudin): A Systematical And Chronological Survey Of The Development From The Fertilized Egg Till The End Of Metamorphosis*, 2nd edition. Amsterdam: North-Holland Publishing Company.

Pai, V. P., Aw, S., Shomrat, T., Lemire, J. M. and Levin, M. (2012). Transmembrane voltage potential controls embryonic eye patterning in *Xenopus laevis*. *Development* **139**, 313-323.

Pasternak, B. and Hviid, A. (2010). Use of proton-pump inhibitors in early pregnancy and the risk of birth defects. *N. Engl. J. Med.* **363**, 2114-2123.

Praetorius, J., Andreasen, D., Jensen, B. L., Ainsworth, M. A., Friis, U. G. and Johansen, T. (2000). NHE1, NHE2, and NHE3 contribute to regulation of intracellular pH in murine duodenal epithelial cells. *Am. J. Physiol.* **278**, G197-G206.

Sabirov, R. Z., Azimov, R. R., Ando-Akatsuka, Y., Miyoshi, T. and Okada, Y. (1999). Na$^+$ sensitivity of ROMK1 K$^+$ channel: role of the Na$^+$/H$^+$ antiporter. *J. Membr. Biol.* **172**, 67-76.

Sasaki, S., Ishibashi, K., Nagai, T. and Marumo, F. (1992). Regulation mechanisms of intracellular pH of *Xenopus laevis* oocyte. *Biochim. Biophys. Acta* **1137**, 45-51.

Sive, H. L., Grainger, R. M. and Harland, R. M. (2000). *Early Development Of Xenopus Laevis: A Laboratory Manual*. Cold Spring Harbor (NY): Cold Spring Harbor Laboratory Press.

Thornton, C. S. (1970). Amphibian limb regeneration and its relation to nerves. *Am. Zool.* **10**, 113-118.

Tseng, A.-S. and Levin, M. (2012). Transducing bioelectric signals into epigenetic pathways during tadpole tail regeneration. *Anat. Rec.* **295**, 1541-1551.

Tseng, A. S., Beane, W. S., Lemire, J. M., Masi, A. and Levin, M. (2010). Induction of vertebrate regeneration by a transient sodium current. *J. Neurosci.* **30**, 13192-13200.

Vandenberg, L. N., Morrie, R. D. and Adams, D. S. (2011). V-ATPase-dependent ectodermal voltage and pH regionalization are required for craniofacial morphogenesis. *Dev. Dyn.* **240**, 1889-1904.

Biology Open

Table S1. Summary of statistical analyses.

Experiment	Measurement	N	Value for dark	Value for light	Test	Value of statistic	*P*
Arch activity	V_{mem}	12	22±8	40±7	t-test	t=3.541	0.002
Arch+YCHE	Craniofacial abnormalities	149	6309	4866	MWU	Z=3.423	<0.001
Arch+stage 47 amputation	Regenerative ability	16	45±24	111±58	t-test	t=3.709	0.002
Arch+stage 47 amputation	Number of H3P-positive cells	22	4±3	12±4	t-test	t=5.237	<0.001
No Arch controls							
No treatment	V_{mem}	6	29±2	29±2	t-test	t=0.346	0.426
YCHE78	Craniofacial abnormalities	105	2665	2901	MWU	Z=−0.67	>0.5
Stage 47 amputation	Regenerative ability	14	69±44	49±30	t-test	t=1.464	0.167